NOLTA, IEICE

Paper

Development of add-on stochastic resonance device for the detection of subthreshold RF signals

Keita Chiga [1 a)], *Hiroya Tanaka* [1], *Takaya Yamazato* [1], *Yukihiro Tadokoro* [2], *and Shintaro Arai* [3]

[1] *Nagoya University, Furo-cho, Chikusa-ku, Nagoya 464-8603, Japan*

[2] *Toyota Central R&D Laboratories, Inc., Aichi 480-1192, Japan*

[3] *National Institute of Technology, Kagawa College, 551 Kohda, Takuma-cho, Mitoyo, Kagawa 769-1192, Japan*

[a)] *chiga@katayama.nuee.nagoya-u.ac.jp*

Received January 24, 2015; Revised April 27, 2015; Published October 1, 2015

Abstract: Stochastic resonance (SR) is a nonlinear phenomenon that, under certain conditions, can enhance system response by adding noise to the signals of some nonlinear system. A particular advantage of SR over conventional linear systems is that it is able to detect subthreshold signals that linear systems hardly sense. Unfortunately, most research of SR in wireless communication systems has focused on fundamental analysis, leaving work to be done in experimental SR research despite the attractiveness of its application. Few attempts have so far addressed the development of SR receivers to show the feasibility of subthreshold signal detection. Those receivers that have been developed are simple ones specially made to confirm the usefulness of SR without needing to support state-of-the-art wireless radio technology. The purpose of this study is to examine the feasibility of using an SR receiver to receive subthreshold radio frequency (RF) signals. A new add-on SR device is developed and confirmation that the SR phenomenon exists within RF is obtained when using software defined radio (SDR) as the post-processing receiver. Furthermore, bit error rate (BER) performance is mainly governed by the add-on SR device's output signal quality.

Key Words: stochastic resonance (SR), stochastic resonance receiver, add-on stochastic resonance device, Schmitt trigger, subthreshold signal detection, subthreshold radio frequency (RF) signal, software defined radio (SDR)

1. Introduction

Stochastic resonance (SR) is an interesting phenomenon in that, under certain conditions, system response can be enhanced by adding independent noise to the signals of some nonlinear systems [1]. Since its discovery by Benzi et al. in 1981, this characteristic has been discussed in the context of nonlinear physics [2, 3] and its application in signal processing has spread to various fields, such as

Nonlinear Theory and Its Applications, IEICE, vol. 6, no. 4, pp. 520–533 DOI: 10.1588/nolta.6.520

signal detection theory [4–6], wireless communication [7–9], and imaging [10].

In the first decade of SR, the fundamental aspects of SR were well discussed in the context of nonlinear physics [11–14]. These works led to the investigation of finding the phenomena in ecological systems [15–17], which motivated the discussion of SR in neural systems [18, 19]. The key component to exhibit SR is nonlinearity, which is observed in optical laser systems [20] and nonlinear material/devices [11, 21]. Since decision-making process in signal processing is also nonlinear operation, signal processing algorithm inherently exhibits SR. In fact, noise benefits have been discussed in hypothesis-testing problems [22, 23], Bayesian estimation [24], and parameter estimation [25].

This paper focuses on SR application in wireless communication.

A particular advantage of SR over conventional linear systems is that it is able to detect a low-level signal that linear systems would hardly sense. In other words, it is able to detect a signal below a receiver's sensitivity. Such a low-level signal is referred to as the subthreshold signal, and it is below the minimum signal level required to achieve a linear system's specific quality. Needless to say, lowering the signal level not only reduces system power consumption but, in some cases, also lowers the amount of systems so that the overall system performance can be improved. Green communications, for instance, is a good example of an area of communication that uses low signals to reduce energy consumption while keeping the emitted interference at a minimum [26].

Unfortunately, much research of SR in wireless communication systems has focused on fundamental analysis [27–29], and experimental SR research is still underway, despite the attractiveness of its application in the field. Barbay et al. have shown experimental results and theoretical analysis of noise-assisted transmission of binary information through a bistable optical system [30]. Studies of the effects of SR in wireless communication systems have suggested that noise, intentionally added to a received signal, could play a prominent role in improving the detection of low signals. In general, it is accepted that SR driven by non-Gaussian noise achieves higher signal processing performance than that obtained by linear systems [31, 32]. For example, in [31] Castro et al. showed that an electronic experimental system had improved performance from SR phenomenon driven by white non-Gaussian noise and Kasai et al. experimentally confirmed the effectiveness of SR in a non-Gaussian environment in [32]. Likewise, Ichiki et al. have shown that it is possible to design a nonlinear estimator to maximize the signal-to-noise ratio (SNR) of the output signal for a given noise [33]. Tanaka et al. have derived a bit error rate (BER) for a subthreshold baseband signal and have shown that the number of samples per symbol, the received signal amplitude, and the receiver sensitivity are three important BER parameters [29].

Few attempts have so far addressed the development of SR receivers to show the feasibility of subthreshold signal detection; the receivers that have been developed are simple ones specially made to confirm the usefulness of SR without needing to support state-of-art wireless radio technology. Hyunju et al. have proposed a signal detection system for communication systems that has been shown to improve the ranger's dynamic range when it is applied [8]. We have implemented a baseband SR receiver and reported that subthreshold signal detection is possible with it [34]. However, these initial studies are still far from practical wireless systems in that they handle baseband signals, not RF signals. Furthermore, they are so simple that synchronization circuits, error correcting code, and other up-to-date circuits are omitted. Thus, a need remains for an actual SR receiver that can not only process a subthreshold RF signal but can also support a modern wireless system.

The subthreshold signal, which is lower than the dynamic range of the system, is difficult to be detected. To solve this problem, traditional approach includes the replacement with the device/system with wide dynamic range, but it needs additional cost. SR is the simple solution because it needs only to add the noise. In the revised manuscript, we added the above comments.

The purpose of this study is to examine the feasibility of using an SR receiver to receive subthreshold RF signals. Our present work not only demonstrates the observation of the stochastic resonance phenomenon in wireless communication systems but also demonstrates stochastic resonance works in conjunction with modern wireless systems. With the help of the stochastic resonance, it is possible to detect a subthreshold RF signal that cannot be received with a conventional RF receiver.

The first contribution of this study is the development of a new add-on SR device and confirmation

that the SR phenomenon exists within RF. The developed device picks up subthreshold RF signals and outputs signals that can be processed by an ordinary wireless receiver. It is composed of an additive noise circuit and Schmitt trigger. More specifically, the input of the add-on SR device is a subthreshold RF signal whose signal level is below the sensitivity of the conventional RF receiver. The device then outputs the signal at a level high enough for the conventional RF receiver to process well. Note that a Schmitt trigger is the simplest two-state system available for the realization of SR [11, 35]. We use the software defined radio (SDR) as our conventional RF receiver, so, generally speaking, any RF signal can be processed.

The second contribution of this study is that BER performance is mainly governed by the output signal quality of the add-on SR device. Since the device's output signal is the SDR receiver's input, one may think that it is obvious that the device's output signal quality governs BER performance. However, the noise circuit and a nonlinear device (the Schmitt trigger in our case) are the key components of the add-on SR device, which means that design of the add-on SR device is not straightforward. We need to consider the device's performance from the perspective of both SR and RF signal reception. To be more specific, the bandwidth of the Schmitt trigger needs to be wide enough to meet the feasibility of using SR with a waveform shaping circuit to generate a desirable output signal. These findings provide the criteria for the design of the add-on SR device.

This paper is organized as follows. In Section 2, we show the system model of the RF SR receiver. We discuss implementation of the SR system for RF in Section 3. Implementation of the SR binary phase shift keying (BPSK) receiver and a performance evaluation of the implemented receiver are shown in Section 4. Conclusions are given in Section 5.

2. System model of the SR receiver system

The system model of the digital wireless communication system applied to the SR phenomenon is shown in Fig. 1. We propose using a conventional RF receiver with the add-on SR device. The conventional RF receiver does not need to be modified. Therefore, the receiver can use conventional synchronization circuits, error correcting code, and other up-to-date circuits. Use of such a receiver provides a simple but effective configuration.

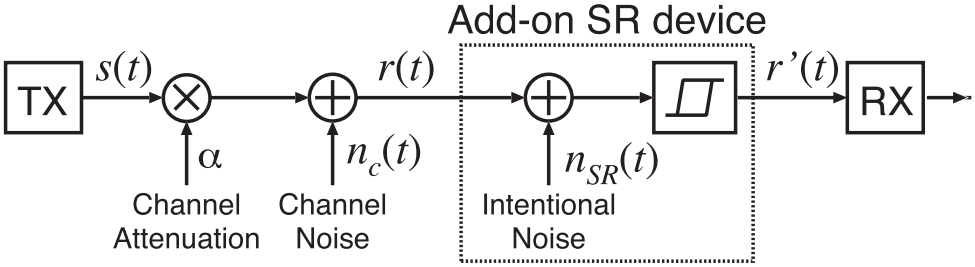

Fig. 1. System model of the RF receiver using the add-on SR device. The add-on SR device composed of an additive intentional noise and Schmitt trigger circuits. The add-on SR device picks up received subthreshold RF signals $r(t)$ and outputs signal $r'(t)$ that can be processed by an ordinary wireless receiver (RX).

The signal $s(t)$ is transmitted by the transmitter TX. This transmitted signal $s(t)$ is propagated to the receiver through the wireless communication channel. Through that channel, the transmitted signal is attenuated by factor α, and channel noise $n_c(t)$ is added to the attenuated signal. In general, channel noise $n_c(t)$ is zero-mean Gaussian noise. Therefore, the received signal $r(t)$ is given by

$$r(t) = \alpha s(t) + n_c(t). \tag{1}$$

In our receiver, the received signal $r(t)$ is input to the add-on SR device. In the add-on SR device, which is composed of the noise circuit and Schmitt trigger, the intentional noise $n_{SR}(t)$ is added to the received signal $r(t)$ in order to optimize the Schmitt trigger's response. We assume that intentional noise $n_{SR}(t)$ is zero-mean Gaussian noise and that its power is adjustable. Therefore, the intentional

noise can adjust the total noise power, allowing us to optimize the Schmitt trigger's system response. The nonlinear circuit (the Schmitt trigger, in our case) detects the signal $s(t)$ from $r(t) + n_{SR}(t)$, and the output of the SR system $r'(t)$ is input to the conventional receiver RX. The conventional receiver RX demodulates and obtains the data bits.

In this system, we assume that the attenuated signal $\alpha s(t)$ is lower than the sensitivity of the conventional receiver η_{RX}. Thus,

$$|\alpha s(t)| < \eta_{RX}. \tag{2}$$

Therefore, if the receiver does not contain the add-on SR device, the receiver cannot detect the signal.

2.1 Schmitt trigger

In order to implement our receiver, the SR circuit that exhibits the SR phenomenon must be implemented. Some electrical circuits are known as the SR circuit [36–38]. In this paper, we use the Schmitt trigger as the SR circuit. The Schmitt trigger can be implemented by a simple circuit [38].

Figure 2 shows the input-output characteristics of the Schmitt trigger as well as an example of the circuit schematic using an op-amp. In Fig. 2, V_i and V_o are the input and output voltage, respectively. The Schmitt trigger has two output voltages V_m and two thresholds η_{SR} that have hysteresis. The Schmitt trigger is the circuit model of the bistable system. The output of the Schmitt trigger $V_o(t)$ is represented as

$$V_o(t) = V_m \ \mathrm{sgn}\left(V_i(t) - \frac{R_1}{R_2} V_o(t - \Delta t)\right), \tag{3}$$

where V_m is the maximum voltage of the output and $V_i(t)$ is the Schmitt trigger's input voltage. Since $V_o(t) \in \{\pm V_m\}$, the threshold of the Schmitt trigger shown in Fig. 2(b) is given by

$$\eta_{SR} = \frac{R_1}{R_2} V_m. \tag{4}$$

In more practical op-amp model or practical circuit, transitioning output $V_o(t)$ has some delay. If the signal frequency is low, we can ignore this delay; however, if the signal frequency is high, we should consider the delay because the Schmitt trigger will not be able to respond to the input. Therefore, we must implement the Schmitt trigger that has a smaller delay when we use the RF signal. In other words, we must implement the Schmitt trigger that has a wider input bandwidth.

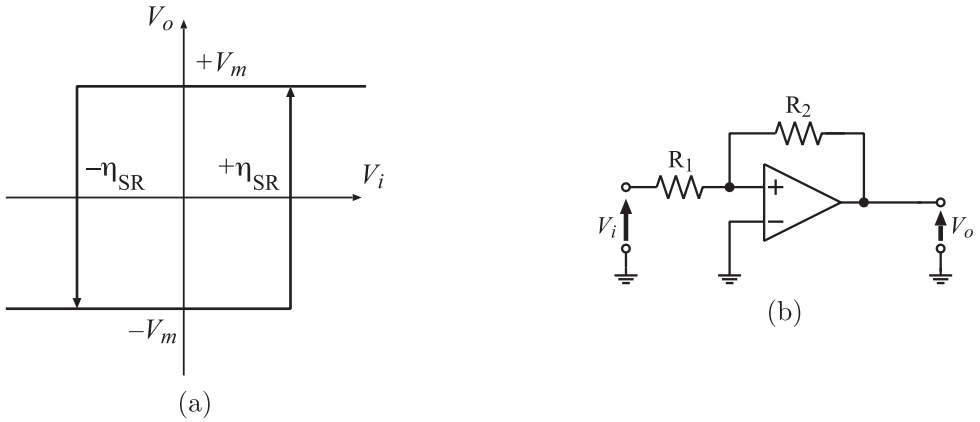

Fig. 2. The input-output characteristic of Schmitt trigger (a) and an example circuit schematic using an op-amp (b). The input voltage is V_i and the output voltage is V_o and the two threshold voltages $\pm\eta_{SR}$ express hysteresis of the Schmitt trigger.

3. The Schmitt trigger for RF signals

In this section, we consider the implementation of the Schmitt trigger which can exhibit the SR in RF. Firstly, we discuss about the required specification of the Schmitt Trigger by introducing the SR in the digital signal processing. Secondly, we implement the Schmitt trigger for RF signals and evaluate its output SNR performance experimentally.

3.1 Required specifications of the Schmitt trigger

In order to discuss about the required specifications of the Schmitt Trigger for RF signals, we introduce the SR in the digital signal processing. In the SR of the digital signal processing, it was reported that the output SNR of the SR system saturates as the sampling frequency increases [39]. The output SNR of the SR system is saturated when $f_{sample} > 5f_c$. If the antialiasing filter is used in the digital signal processing, the signal components which has higher frequency than the cutoff frequency are removed. In generally, the cutoff frequency of the antialiasing filter is $f_{sample}/2$. Hence, the signal has the components lower than the $f_{sample}/2$. On the other hand, the input of the Schmitt trigger has the signal components within its input bandwidth W_{SR}. Generally, the lower end of the input bandwidth of the Schmitt trigger is 0Hz. Because of these characteristics, We can set the sampling frequency of the digital signal processing f_{sample} with the input bandwidth of the Schmitt trigger W_{SR} as follows.

$$f_{sample} = \frac{1}{2} W_{SR} > 5f_c \tag{5}$$

Therefore, the required input bandwidth of the Schmitt trigger is

$$W_{SR} > 10f_c. \tag{6}$$

The condition of exhibiting SR has been discussed in terms of transition rate in double-well potential systems, where the signal frequency is much smaller than this rate [2]. A Schmitt trigger is one realization of the system, and hence, the input bandwidth WSR in the Schmitt trigger, which is equal to this rate, should meet the condition: $W_{SR} \gg f_c$. Our result of $W_{SR} > 10f_c$ in Eq. (6) satisfies this condition.

It is known that the adding noise $n_c(t) + n_{SR}(t)$ could play a prominent role for SR. In most of the study of the SR, the bandwidth of the input noise W_N is assumed to be white. However, in the experiment, the generation of the white noise is difficult. We note that the Schmitt trigger cannot respond to the signal component whose frequency is outside of the bandwidth. Therefore, the bandwidth of the noise W_N is necessary to be as wide as possible within the bandwidth of Schmitt trigger W_{SR}.

3.2 The implementation of the Schmitt trigger

From above discussion, we implement the Schmitt trigger which exhibit the SR in RF. We assume that the signal frequency is 50 MHz, so the required input bandwidth is about 500 MHz. We implemented the Schmitt trigger using the high speed comparator (Analog Devices ADCMP607) whose input bandwidth is 750 MHz. The circuit schematic and the snapshot of our implemented Schmitt trigger are shown in Fig. 3. In order to remove the influence of unintentional noise, we shielded the implemented circuit in the metal case.

We experimentally evaluate the output SNR performance of our implemented Schmitt trigger. The purpose of the output SNR evaluation is the confirmation of the SR phenomenon of the circuit. The sinusoidal signal $\alpha s(t)$ whose amplitude is under the threshold of the Schmitt Trigger is supposed as the input. The channel noise $n_c(t)$ is assumed to be negligibly small. If the noise power of the intentional noise $n_{SR}(t)$ is zero, the input signal cannot exceed the threshold and cannot be detected. The experimental parameters and the measurement system are shown in Table I and Fig. 4 respectively. We measure the output SNR of the Schmitt trigger as a function of its input noise Power Spectrum Density (PSD). The signal source (Agilent Technologies 33250A) generates the sinusoidal signal $\alpha s(t)$ whose frequency is 14 MHz and the noise $n_{SR}(t)$ from the noise source (Agilent Technologies N5182A) is added to the signal $\alpha s(t)$. Then, the corrupted signal $\alpha s(t) + n_{SR}(t)$ is input to the Schmitt trigger. The output of the Schmitt trigger is fed into the Analog to Digital Converter (Thinknet DF-4000), and the output SNR is calculated. These instruments are connected by the coaxial cable. The output SNR γ is given by

$$\gamma = 10 \log_{10} \frac{S(\omega_s)}{S_N}, \tag{7}$$

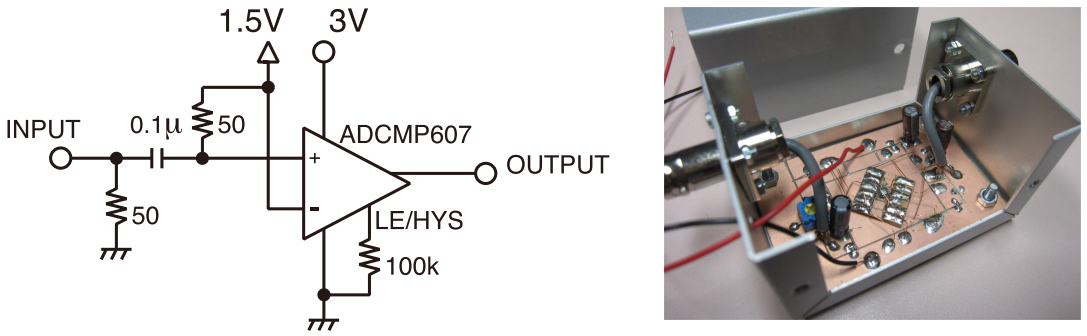

(a) (b)

Fig. 3. The circuit schematic of our implemented Schmitt trigger (a) and its snapshot (b). We implemented the Schmitt trigger using a high speed comparator (Analog Devices ADCMP607) whose input bandwidth is 750 MHz. The threshold of the Schmitt trigger η_{SR} is 100 mV.

Table I. The measurement parameters of the output SNR.

Signal waveform	Sinusoidal
Signal frequency f_c	14 MHz
Signal amplitude A	80 mV
Threshold of Schmitt trigger η_{SR}	100 mV
Noise distribution	Gaussian
Noise bandwidthW_N	100 MHz
Sampling frequency f_{sample}	100 MHz
Total Measurement time per trial	0.17 ms
Number of trial	10

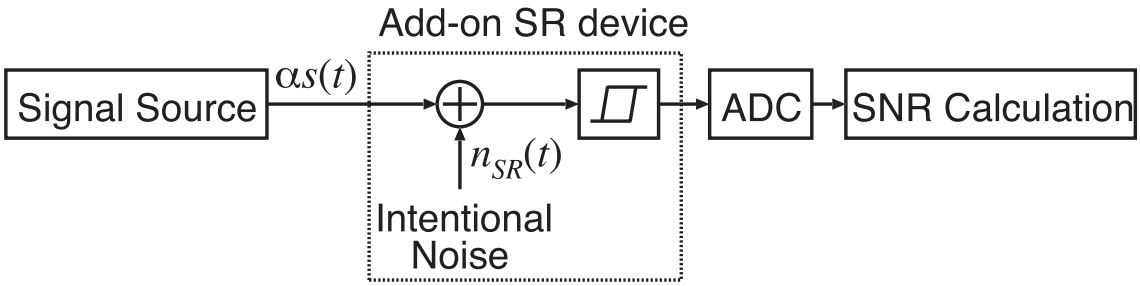

Fig. 4. The measurement system of the output SNR of the Schmitt trigger. The parameters are summarized in Table I. We generated a sinusoidal signal $\alpha s(t)$ by Agilent Technologies 33250A Function/Arbitrary Waveform Generator and added intentional noise $n_{SR}(t)$ generated by Agilent Technologies N5182A MXG Vector Signal Generator. The corrupted signal $\alpha s(t) + \eta SR(t)$ is input to the implemented Schmitt trigger. Note that the signal amplitude is 80 mV, which is lower than the threshold of the Schmitt trigger, 100 mV. The output of the Schmitt trigger is fed into an analog to digital converter (Thinknet DF-4000) and the output SNR is calculated.

where $S(\omega_s)$ is the PSD at the signal frequency, and S_N is the average noise PSD around the signal frequency.

The experimental result is shown in Fig. 5. The result of the conventional add-on SR device using the Schmitt trigger whose input bandwidth is 140 MHz is also shown in Fig. 5. The conventional Schmitt trigger is implemented by the high speed op-amp (Texas Instruments LM7171). In this figure, the horizontal axis is the noise PSD generated by the noise source, and the vertical axis is the output SNR of the Schmitt Trigger. From this figure, the output SNR of the conventional add-on SR device has no peak, but the output SNR of our proposed add-on SR device has a peak at PSD = $10^{-11}\mathrm{V}^2/\mathrm{Hz}$. Therefore, we confirmed that the bandwidth of the Schmitt trigger must be ten times higher than that of the RF signal and the value of the input noise PSD needs to be optimally chosen.

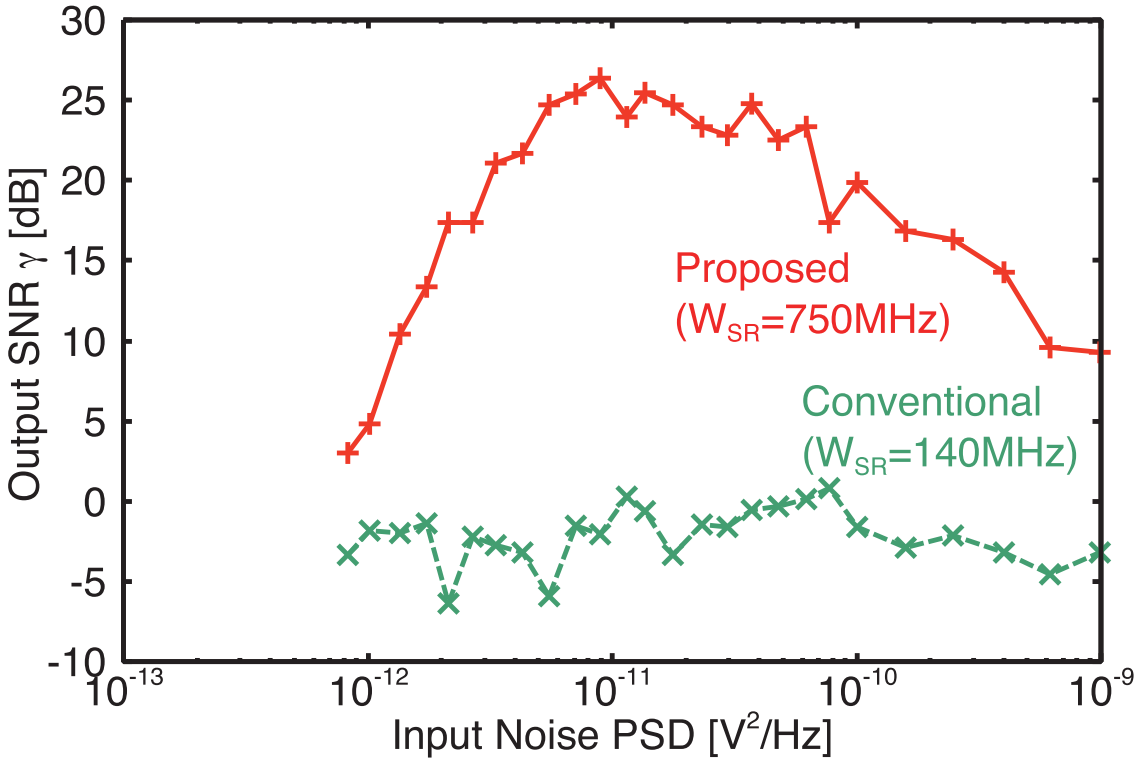

Fig. 5. The output SNR performance of the implemented add-on SR device for two different Schmitt trigger circuits. The curve indicated "Proposed" is the case of the Schmitt trigger implemented by the high speed comparator (Analog Devices ADCMP607) whose input bandwidth is 750 MHz. While the curve indicated "Conventional" is the case of the Schmitt trigger implemented by the high speed op-amp (Texas Instruments LM7171) whose input bandwidth is 140 MHz. As the required input bandwidth of the add-on SR device is 500 MHz for 50 MHz signal, we observe degradation in output SNR of the conventional one ($W_{SR} = 140$ MHz).

4. The implementation of the BPSK receiver using SR

In this paper, we consider the application of the SR phenomenon to the BPSK receiver. The Schmitt trigger has the optimal input noise PSD. It is known that the optimal noise PSD is depend on the difference between the amplitude of the input signal and the threshold of the Schmitt trigger. In generally, the threshold of the Schmitt trigger is constant. If the variation of the signal amplitude is too large, the optimal noise PSD is varied and the add-on SR device may not detect the signal. So, we consider the BPSK signal since its amplitude is constant.

The system model of our SR BPSK receiver is shown in Fig. 6. This receiver is composed of the add-on SR device and the conventional BPSK receiver. In the add-on SR device, the intentional noise $n_{SR}(t)$ is added to the received signal $r(t)$ to optimize the noise PSD. In the conventional BPSK receiver, the output of the Schmitt trigger $r'(t)$ is downconverted to the baseband signal by the mixer and the LPF. The baseband signal is decided by the BPSK detector and the received data is obtained. The conventional BPSK receiver is required to implement this SR BPSK receiver.

4.1 Implementation of BPSK receiver with SDR

We consider the implementation of the conventional BPSK receiver with SDR. The SDR receiver processes most of demodulation processing by the digital signal processing. There are two advantages of the SDR receiver. Firstly, we only have to change its program or software in order to change the demodulation processing. Generally speaking, the SDR receiver can process any RF signal by changing its software. Therefore, we can easily modify our receiver so that it can use any modulation scheme and frequency. Secondly, the SDR receiver has more stability than the analog receiver. For these reasons, we use a SDR receiver as the conventional BPSK receiver.

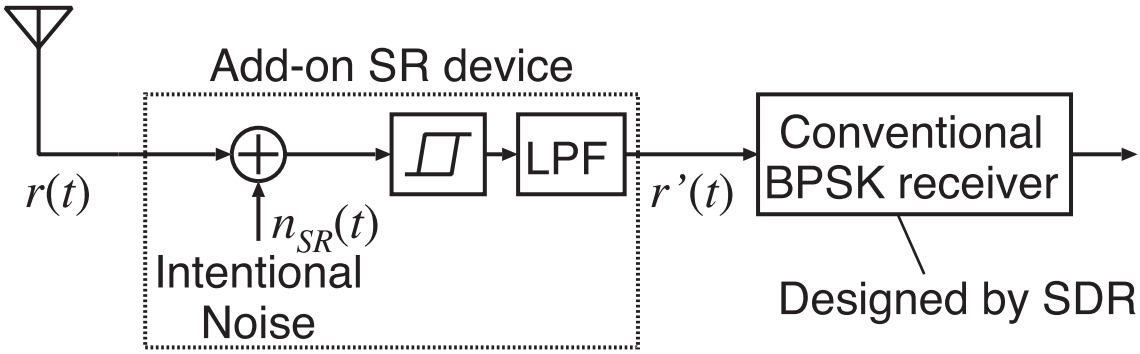

Fig. 6. The system model of our BPSK receiver using the add-on SR device. For the conventional BPSK receiver, we use National Instruments USRP-2920 software-programmable radio transceivers as the hardware of the receiving system.

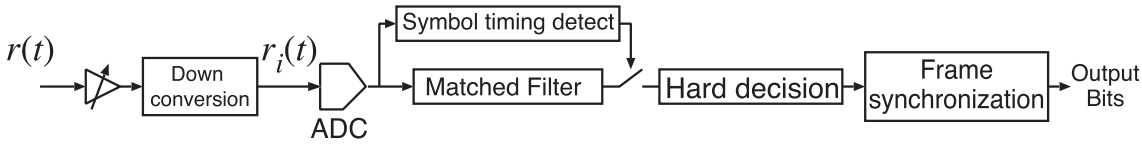

Fig. 7. The system model of the BPSK demodulation system. The system is designed by National Instruments LabVIEW and operated by National Instruments USRP-2920 software-programmable radio transceivers.

Figure 7 shows the system model of our implemented BPSK receiver. Initially, the received RF signal $r(t)$ is received. The received BPSK signal through the wireless channel is given by

$$r(t) = s(t) + n_c(t) = \sum_{i=0}^{n} (2a_i - 1)g(t - iT)\cos(2\pi f_c t) + n_c(t), \tag{8}$$

where $a_i \in \{0, 1\}$ is the transmitted data bits, $g(t)$ represents a pulse of duration T, f_c is the carrier frequency and $n_c(t)$ is the channel noise. The received RF signal $r(t)$ is downconverted to the baseband signal $r_l(t)$ given by

$$r_l(t) = s_l(t) + n_{cl}(t) = \sum_{i=0}^{n} (2a_i - 1)g(t - iT) + n_{cl}(t), \tag{9}$$

where $n_{cl}(t)$ is the downconverted channel noise. The ADC convert the continuance baseband signal $r_l(t)$ to discrete time sequence $r_l[m]$.

$$r_l[m] = r_l\left(\frac{m}{f_{sample}}\right). \tag{10}$$

The sampled sequence $r_l[m]$ is input to the matched filter which is implemented by FIR filter. The impulse response of the FIR filter $h(t)$ is given by

$$h(t) = s(T - t). \tag{11}$$

At the same time, the symbol timing is detected. The output of the matched filter is sampled at the symbol timing and the symbol is decided by the hard decision. The synchronization bits is used in the frame synchronization processing. Finally, the data bits a_i is obtained.

We use USRP-2920 (National Instruments) as the hardware of the receiving system.

4.2 LPF to remove the harmonics

In this paper, we use the Schmitt trigger as the SR circuit. The problem in using a Schmitt trigger is that the output waveform of the Schmitt trigger has many harmonics (see 4.3.3 for evaluation result of the Schmitt trigger output waveform). These harmonics deteriorate the performance of the receiver.

Thus, we consider removing the harmonics using a low pass filter (LPF). The PSD of BPSK signal is given by

$$G_s(f) = \frac{P_s T}{2} \left\{ \left[\frac{\sin\left(\pi(f - f_c)T\right)}{\pi(f - f_c)T} \right]^2 + \left[\frac{\sin\left(\pi(f + f_c)T\right)}{\pi(f + f_c)T} \right]^2 \right\}, \tag{12}$$

where P_s is the signal power, T is the symbol duration and f_c is the carrier frequency. On the other hand, The PSD of BPSK signal through the Schmitt trigger is

$$G'_s(f) = \sum_{n=1}^{\infty} \frac{4{V_m}^2}{\pi^2(2n-1)^2} \left\{ \left[\frac{\sin\left(\pi(f \pm nf_c)T\right)}{\pi(f - \pm nf_c)T} \right]^2 \right\}. \tag{13}$$

From this equation, the output of the Schmitt trigger has the harmonics whose center frequency is nf_c, where n is an integer, $n > 1$. In order to remove these harmonics, we insert the LPF between the Schmitt trigger and the BPSK demodulation system. Since we assume the signal frequency is 50 MHz, we set the cutoff frequency of the LPF to 70 MHz.

4.3 Evaluation of the BER performance

4.3.1 Measurement setup

We evaluate the performance of our implemented SR BPSK receiver. Table II and Fig. 8 show the experimental parameters and the measurement system respectively.

Table II. The measurement parameters of the BER.

Modulation scheme	Binary PSK
Carrier Frequency f_c	50 MHz
Signal Amplitude A	80 mV
Threshold of Schmitt trigger η_{SR}	100 mV
Noise distribution	Gaussian
Noise bandwidthW_N	100 MHz
Sampling frequency f_{sample}	100 MHz
Data bits per frame	1000
Total Measurement time per trial	1.08 ms
Number of trial	100

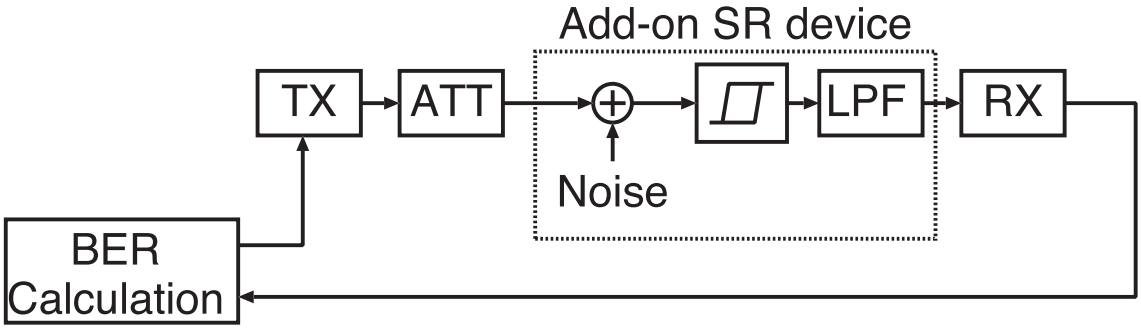

Fig. 8. The measurement system of our BPSK receiver using the add-on SR device. The transmitter signal is BPSK whose center frequency is 50 MHz. The signal is attenuated and white Gaussian noise is added, which is generated by Agilent Technologies N5182A MXG Vector Signal Generator. The signal is then fed into the Schmitt trigger circuit. The output signal of the Schmitt trigger passes through the LPF and conventional BPSK demodulation is performed. Finally, BER is calculated.

We use the BPSK signal whose frequency is 50 MHz as the transmitted signal. In the transmitter TX, the pseudorandom data is modulated and transmitted. This transmitted signal is attenuated by the attenuator ATT so that the received signal becomes subthreshold. Then, the noise from the noise source (Agilent Technologies N5182A) is added to the attenuated signal, and they are inputted

to the Schmitt trigger. The output of the Schmitt trigger pass through the LPF. These instruments are connected by the coaxial cable. The conventional BPSK receiver RX demodulates and decides the data bits. Finally, we compare between the transmitted data bits and the received data bits, and its BER is calculated.

4.3.2 BER perfromance

The experimental results are shown in Fig. 9. In this figure, the horizontal axis is the input noise PSD and the vertical axis is BER. The solid line is the result using the LPF, and the dashed line is the result without the LPF.

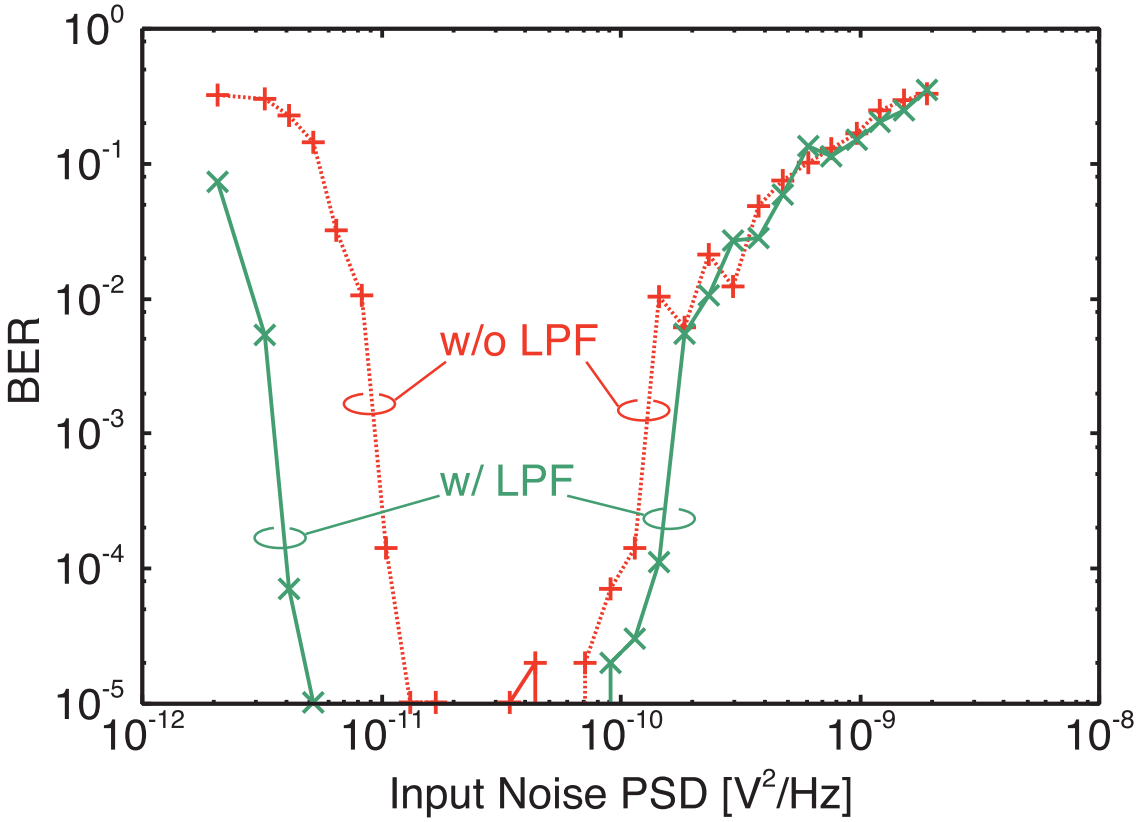

Fig. 9. The input noise PSD versus Bit Error Rate performance. The enhancement of the BER performance by the SR phenomenon using the implemented add-on SR device is confirmed. Furthermore, the use of the LPF after the Schmitt trigger circuit is essential in BER improvement.

Figure 9 shows that the optimal value of the input noise PSD can enhance the BER. The optimal value of the input noise PSD is about $2 \times 10^{-11}\mathrm{V}^2/\mathrm{Hz}$. This value is same as the optimal value of the output SNR of the add-on SR device. Therefore, the enhancement of the BER performance is caused by the SR phenomenon, and our implemented add-on SR device exhibits the SR phenomenon in RF even using the conventional SDR as a post-processing receiver.

4.3.3 Effect of LPF

Furthermore, in Fig. 9, it is shown that the BER performance of the receiver using the LPF is higher than that of the receiver without the LPF. From this result, the LPF which removes the harmonics can improve the BER performance. Figure 10 shows the output waveform of the Schmitt trigger and the output of the LPF. In this figure, the dashed line is the output of the Schmitt trigger and the solid line is the output of the LPF. The output of the LPF becomes sinusoidal. We can see the effect of the LPF in terms of its time waveform. Figure 11 shows the PSDs of the output of the Schmitt trigger and the output of the LPF. As you can see, the PSD of the output of the Schmitt trigger has the harmonics at 100 MHz and 150 MHz. But the PSD of the output of the LPF has only signal

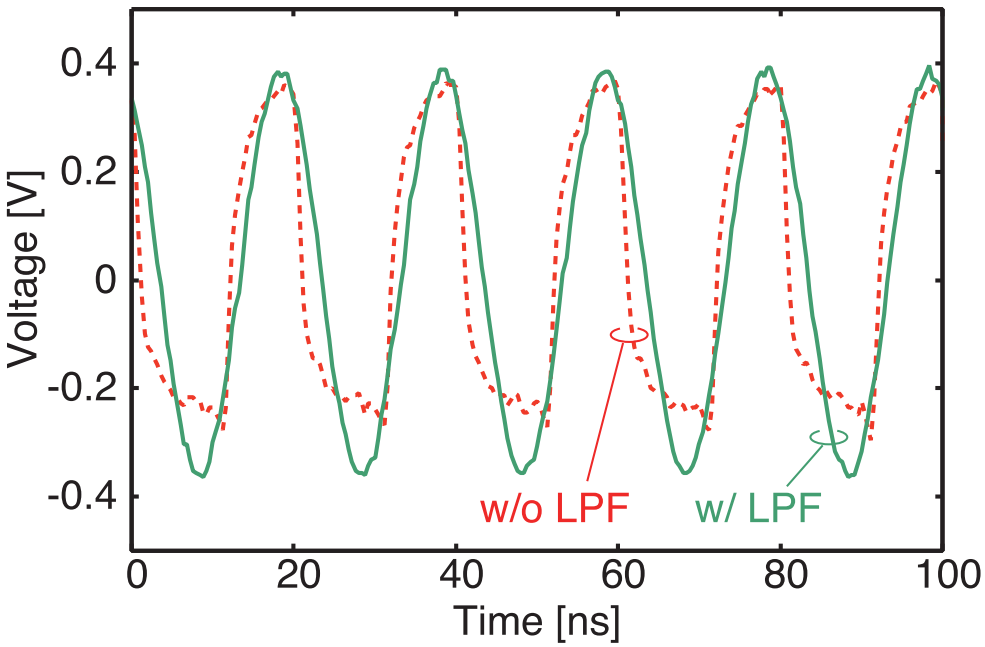

Fig. 10. The output waveform of Schmitt trigger with and without LPF. Without the LPF, a distortion in the output signal is confirmed because of harmonics of the Schmidt trigger output waveform.

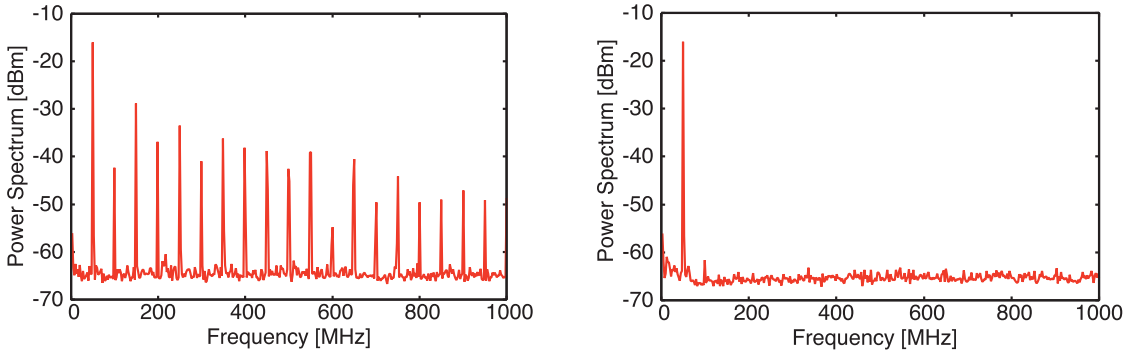

Fig. 11. The PSD of the Schmitt trigger output without LPF (a) and with LPF (b). Since the Schmitt trigger output signal has rectangular pulses, harmonics on PSD are observed for the case without the LPF. If we reduce the harmonics by the LPF, we generate a single peak in PSD, resulting in a sinusoidal signal, as shown in Fig. 9.

component. From this result, we can confirm the effect of the LPF in terms of the frequency domain. We have shown that the BER performance of our receiver is dominated by the quality of the output signal of the add-on SR device.

5. Conclusions

In this study, we have discussed the feasibility of using an SR receiver to detect subthreshold RF signal. We have shown that our newly developed add-on SR device exhibits the SR phenomenon in RF even when using conventional SDR as the post-processing receiver. Our results show definite promise for applying SR to wireless communication systems. Based on our findings, the add-on SR device (which consists of an additive noise circuit followed by the Schmidt trigger) provides a simple but effective configuration. We have shown that the device's bandwidth must be ten times higher than that of the RF signal and that noise variance needs to be optimally chosen to support the SR phenomenon. Furthermore, the quality of add-on SR device's output signal dominates BER performance. Thus, waveform shaping by the LPF is mandatory for removing the harmonics contained in the Schmitt

trigger circuit's output.

Acknowledgments

The authors would like to thank Prof. Masaaki KATAYAMA of Nagoya University, Associate Prof. Hiraku OKADA of Nagoya University, and Assistant Prof. Kentaro KOBAYASHI of Nagoya University for their variable suggestions. A part of this work is supported by KAKENHI, Grant-in-Aid for Scientific Research 26630174.

References

[1] R. Benzi, A. Sutera, and A. Vulpiani, "The mechanism of stochastic resonance," *Journal of Physics A: Mathematical and General*, vol. 14, no. 11, p. L453, 1981. [Online]. Available: http://stacks.iop.org/0305-4470/14/i=11/a=006

[2] L. Gammaitoni, P. Hänggi, P. Jung, and F. Marchesoni, "Stochastic resonance," *Rev. Mod. Phys*, vol. 70, no. 1, pp. 223–287, January 1998.

[3] A. Ichiki, Y. Tadokoro, and M.I. Dykman, "Singular probability distribution of shot-noise driven systems," *Phys. Rev. E*, vol. 87, p. 012119, January 2013. [Online]. Available: http://link.aps.org/doi/10.1103/PhysRevE.87.012119

[4] F.C. Blondeau and D. Rousseau, "Noise-enhanced performance for an optimal bayesian estimator," *Signal Processing, IEEE Transactions on*, vol. 52, no. 5, pp. 1327–1334, May 2004.

[5] S. Kay, "Can detectability be improved by adding noise?" *Signal Processing Letters, IEEE*, vol. 7, no. 1, pp. 8–10, January 2000.

[6] A. Patel and B. Kosko, "Optimal noise benefits in neyman-pearson and inequality-constrained statistical signal detection," *Signal Processing, IEEE Transactions on*, vol. 57, no. 5, pp. 1655–1669, May 2009.

[7] D. He, Y. Lin, C. He, and L. Jiang, "A novel spectrum-sensing technique in cognitive radio based on stochastic resonance," *Vehicular Technology, IEEE Transactions on*, vol. 59, no. 4, pp. 1680–1688, May 2010.

[8] H. Ham, T. Matsuoka, and K. Taniguchi, "Application of noise-enhanced detection of subthreshold signals for communication systems," *IEICE Trans. Fundamentals*, vol. E92-A, no. 4, pp. 1012–1018, April 2009.

[9] S. Sugiura, A. Ichiki, and Y. Tadokoro, "Stochastic-resonance based iterative detection for serially-concatenated turbo codes," *Signal Processing Letters, IEEE*, vol. 19, no. 10, pp. 655–658, October 2012.

[10] M. Dykman, D. Luchinsky, R. Mannella, P. McClintock, N. Stein, and N. Stocks, "Stochastic resonance in perspective," *Il Nuovo Cimento D*, vol. 17, no. 7-8, pp. 661–683, 1995. [Online]. Available: http://dx.doi.org/10.1007/BF02451825

[11] B. McNamara and K. Wiesenfeld, "Theory of stochastic resonance," *Phys. Rev. A*, vol. 39, pp. 4854–4869, May 1989. [Online]. Available: http://link.aps.org/doi/10.1103/PhysRevA.39.4854

[12] M.I. Dykman, R. Mannella, P.V.E. McClintock, and N.G. Stocks, "Phase shifts in stochastic resonance," *Phys. Rev. Lett.*, vol. 68, pp. 2985–2988, May 1992.

[13] J.J. Collins, C.C. Chow, A.C. Capela, and T.T. Imhoff, "Aperiodic stochastic resonance," *Phys. Rev. E*, vol. 54, pp. 5575–5584, November 1996. [Online]. Available: http://link.aps.org/doi/10.1103/PhysRevE.54.5575

[14] L. Gammaitoni, P. Hänggi, P. Jung, and F. Marchesoni, "Stochastic resonance," *Rev. Mod. Phys.*, vol. 70, pp. 223–287, January 1998. [Online]. Available: http://link.aps.org/doi/10.1103/RevModPhys.70.223

[15] K. Wiesenfeld and F. Moss, "Stochastic resonance and the benefits of noise: from ice ages to crayfish and squids," *Nature*, vol. 373, no. 6509, pp. 33–36, January 1995. [Online]. Available: http://dx.doi.org/10.1038/373033a0

[16] J.J. Collins, C.C. Chow, and T.T. Imhoff, "Stochastic resonance without tuning," *Nature*, vol. 376, no. 6537, pp. 236–238, July 1995. [Online]. Available: http://dx.doi.org/10.1038/376236a0

[17] D.F. Russell, L.A. Wilkens, and F. Moss, "Use of behavioural stochastic resonance by paddle fish for feeding," *Nature*, vol. 402, no. 6759, pp. 291–294, November 1999. [Online]. Available: http://dx.doi.org/10.1038/46279

[18] B. Kosko and S. Mitaim, "Stochastic resonance in noisy threshold neurons," *Neural Networks*, vol. 16, no. 5–6, pp. 755–761, 2003, advances in Neural Networks Research: {IJCNN} '03. [Online]. Available: http://www.sciencedirect.com/science/article/pii/S089360800300128X

[19] S. Mitaim and B. Kosko, "Adaptive stochastic resonance," *Proceedings of the IEEE*, vol. 86, no. 11, pp. 2152–2183, November 1998.

[20] M.I. Dykman, G.P. Golubev, I.K. Kaufman, D.G. Luchinsky, P.V.E. McClintock, and E.A. Zhukov, "Noise-enhanced optical heterodyning in an all-optical bistable system," *Applied Physics Letters*, vol. 67, no. 3, pp. 308–310, 1995.

[21] S. Kasai and T. Asai, "Stochastic resonance in schottky wrap gate-controlled gaas nanowire field-effect transistors and their networks," *Applied Physics Express*, vol. 1, no. 8, p. 083001, 2008. [Online]. Available: http://stacks.iop.org/1882-0786/1/i=8/a=083001

[22] S. Bayram and S. Gezici, "Stochastic resonance in binary composite hypothesis-testing problems in the neyman – pearson framework," *Digital Signal Processing*, vol. 22, no. 3, pp. 391–406, 2012. [Online]. Available: http://www.sciencedirect.com/science/article/pii/S1051200412000371

[23] F.C. Blondeau and D. Rousseau, "Raising the noise to improve performance in optimal processing," *Journal of Statistical Mechanics: Theory and Experiment*, vol. 2009, no. 01, p. P01003, 2009. [Online]. Available: http://stacks.iop.org/1742-5468/2009/i=01/a=P01003

[24] ——, "Noise-enhanced performance for an optimal bayesian estimator," *Signal Processing, IEEE Transactions on*, vol. 52, no. 5, pp. 1327–1334, May 2004.

[25] H. Chen, P. Varshney, and J. Michels, "Noise enhanced parameter estimation," *Signal Processing, IEEE Transactions on*, vol. 56, no. 10, pp. 5074–5081, October 2008.

[26] G. Gür and F. Alagöz, "Green wireless communications via cognitive dimension: an overview," *Network, IEEE*, vol. 25, no. 2, pp. 50–56, March 2011.

[27] H. Tanaka, T. Yamazato, and S. Arai, "Preliminary study on bpsk receiver using stochastic resonance," *2012 RISP International Workshop on Nonlinear Circuits, Communications and Signal Processing*, pp. 64–67, March 2012.

[28] H. Tanaka, K. Chiga, T. Yamazato, T. Y, and S. Arai, "Performance evaluation of stochastic resonance receiver for the multi carrier detection," *NANOENERGY2013*, pp. 58–59, July 2013.

[29] H. Tanaka, K. Chiga, T. Yamazato, Y. Tadokoro, and S. Arai, "An analysis method of a stochastic resonance receiver using a schmitt trigger," *NOLTA'14*, pp. 193–196, September 2014.

[30] S. Barbay, G. Giacomelli, and F. Marin, "Noise-assisted transmission of binary information: Theory and experiment," *Phys. Rev. E*, vol. 63, p. 051110, April 2001. [Online]. Available: http://link.aps.org/doi/10.1103/PhysRevE.63.051110

[31] F.J. Castro, M.N. Kuperman, M. Fuentes, and H.S. Wio, "Experimental evidence of stochastic resonance without tuning due to non-gaussian noises," *Phys. Rev. E*, vol. 64, p. 051105, October 2001. [Online]. Available: http://link.aps.org/doi/10.1103/PhysRevE.64.051105

[32] S. Kasai, Y. Tadokoro, and A. Ichiki, "Design and characterization of nonlinear functions for the transmission of a small signal with non-gaussian noise," *Phys. Rev. E*, vol. 88, p. 062127, December 2013. [Online]. Available: http://link.aps.org/doi/10.1103/PhysRevE.88.062127

[33] A. Ichiki and Y. Tadokoro, "Relation between optimal nonlinearity and non-gaussian noise: Enhancing a weak signal in a nonlinear system," *Phys. Rev. E*, vol. 87, p. 012124, January 2013. [Online]. Available: http://link.aps.org/doi/10.1103/PhysRevE.87.012124

[34] K. Chiga, H. Tanaka, T. Yamazato, Y. Tadokoro, and S. Arai, "Implementation of bi-polar pulse sr receiver using schmitt trigger and evaluation of its performance," *Proc. NOLTA'13*, pp. 269–271, September 2013.

[35] V.I. Melnikov, "Schmitt trigger: A solvable model of stochastic resonance," *Phys. Rev. E*, vol. 48, pp. 2481–2489, October 1993. [Online]. Available: http://link.aps.org/doi/10.1103/PhysRevE.48.2481

[36] D. Luchinsky, R. Mannella, P. McClintock, and N. Stocks, "Stochastic resonance in electrical circuits. ii. nonconventional stochastic resonance," *Circuits and Systems II: Analog and Digital Signal Processing, IEEE Transactions on*, vol. 46, no. 9, pp. 1215–1224, September 1999.

[37] ——, "Stochastic resonance in electrical circuits. ii. nonconventional stochastic resonance," *Circuits and Systems II: Analog and Digital Signal Processing, IEEE Transactions on*, vol. 46, no. 9, pp. 1215–1224, September 1999.

[38] G. Harmer, B. Davis, and D. Abbott, "A review of stochastic resonance: circuits and measurement," *Instrumentation and Measurement, IEEE Transactions on*, vol. 51, no. 2, pp. 299–309, April 2002.

[39] A. Ichiki, Y. Tadokoro, and M. Takanashi, "Sampling frequency analysis for efficient stochastic resonance in digital signal processing," *J. Sig. Process*, vol. 16, no. 6, pp. 467–475, November 2012.